AIDIC *Conference Series*, Vol. 9, 2009
Editor Sauro Pierucci
DOI: 10.3303/ACOS0909042

ISBN 978-88-95608-10-5 ISSN 2036-5969

LOADED NANOPARTICLES WITH HYDROPHOBIC CYANINES: PREPARATION, CHARACTERIZATION AND ENCAPSULATION

Kazimiera A. Wilk[a], Katarzyna Zielińska[a], Jadwiga Pietkiewicz[b], Jolanta Saczko[b]

[a]Department of Chemistry, Wroclaw University of Technology,
Wybrzeże Wyspiańskiego 27, 50-370 Wrocław, Poland
[b]Department of Medical Biochemistry, Medical University of Wroclaw,
Chalubinskiego 10, 50-368 Wroclaw, Poland

The aim of the present contribution was to prepare poly(*n*-butyl cyanoacrylate) hollow nanocapsules, loaded with cyanine-type hydrophobic photosensitizers such as IR-768, IR-780 and IR-783 cyanines, by means of interfacial polymerization in oil-in-water (o/w) microemulsions. The microemulsion templates were prepared in situ using nonionic surfactants, such as Tween 80 and Brij 96. *Iso*-propylmyristate was used as the cyanine solubilizing locus (i.e., the oil phase), whereas *iso*-propanol - as the cosurfactant. The entrapment of the selected compounds - potential photosensitizers - determined indirectly by detecting the concentration of the remaining cyanine in the supernatant following the isolation process of the nanoparticles - was achieved in the range of 60-90% for each studied cyanine. The cyanine-loaded nanoparticles were visualized by images taken with atomic force microscopy (AFM) and scanning electron microscopy (SEM). They were spherical in shape with radii of 111 to 420 nm ± 2.5 nm and highly monodispersive in most cases. The nanocapsules dimensions were dependent on the polymeric envelope thickness as revealed by dynamic light scattering (DLS), AFM and SEM.

1. INTRODUCTION

Surfactant-oil-water systems may be used as templates to produce nanostructured materials, as delivery vehicles for drugs and food additives, and as solvents in: degreasing, cleaning, bio-separations, polymerization, environmental remediation, and enhanced oil recovery (Gasco et al., 1986; Date et al., 2008). Among many micellar aggregates and their mediated systems, polymeric nanoparticles have been designed to successfully encapsulate hydrophobic drugs in order to target cells and avoid drug degradation and toxicity as well as to improve drug efficacy (Allemann et al., 1993; Couvreur et al., 2002). In particular, hollow nanocapsules consisting of a liquid core in a thin polymer envelope obtained via interfacial polymerization have received special interest as one of the most potential polymer - based colloidal drug delivery systems (Guterres et al., 2007). After parenteral administration, the penetration extent and transport range of nanocapsules from the blood to the target tissue depend, inter alia, on the size of these drug carriers. Due to their molecular size, ranging between 100-700 nm, the nanocapsules escape renal clearance and have prolonged serum half-life period. Often they cannot penetrate the endothelial junctions of normal blood vessels. But vascular endothelium in pathological sites (solid tumors, inflammation tissues and infracted areas) is discontinuous with large fenestrations of 200-780 nm, which allow the nanoparticle passage (Gaumet et al., 2008). In particular, broad efforts are headed to design effective delivery systems for anticancer drugs which should be selectively retained by malignant tissue. Generally, it is expected that the most applicable drug delivery system should be biodegradable, biocompatible, and unassociated with incidental adverse effects. Furthermore, it is very important to achieve the lowest possible cytotoxicity of empty nanocarriers constructed for cancer cells and to obtain the therapeutic effect only by having the bioactive substance delivered in nanoparticle entities. One of the striking examples here is the photodynamic therapy (PDT) - considered as a treatment modality in oncology - it uses a combination of light and photosensitizers to cause cancer cellular and tissue damages (Castano et al., 2004; Crescenzi et al., 2004). In clinical PDT however, the same side effects were observed as a result of dark toxicity of photosensitizers towards cancer and normal cells (Castano et al., 2004). For this reason, the

Please cite this article as: Wilk K.A., Zielinska K., Pietkiewicz J. and Saczko J., (2009), Loaded nanoparticles with cyanine-type photosensitizers: preparation, characterization and encapsulation, AIDIC Conference Series, 09, 365-372
DOI: 10.3303/ACOS0909042

incorporation of such hydrophobic molecules into biocompatible nanocapsules may reduce cytotoxicity of a free photosensitizer and permit to deliver greater amounts of them to the cancer cells. In the present work we continue our search for the most desirable microemulsion-templated hollow nanostructures for the hydrophobic photosensitizer encapsulation. Previously, we have report the successfully encapsulation of the cyanine IR-768 molecules in sugar surfactant microemulsion-templated nanocapsules, which being internalized in MCF-7 breast cancer cells, effectively enhanced cell death after light irradiation (Zielinska, 2008b). At present our interest is focused on the encapsulation of cyanine IR-768, IR-780 and IR-783 dyes in polymeric nanocapsules, prepared in nonionic microemulsion–templated processes to be further studied as potent photosensitizer molecules to the cancer cells in the photodynamic therapy (PDT).

2. EXPERIMENTAL

2.1. Materials

All reagents were of analytical grade and used as provided. Most chemicals were purchased from Sigma-Aldrich, i.e., the polyoxyethyleneted nonionics: Tween 80 (Polysorbate 80) - polyoxyethylene 20 sorbitan mono-oleate and Brij 96 - polyoxyethylene 10 oleyl ether, chloroform, ethanol, dimethylsulfoxide (DMSO), Dulbecco's Modified Eagle medium (DMEM), cyanine IR-768, IR-780 and IR-783, *iso*-propanol IP (as cosurfactant). *iso*-Propylmyristate IPM (from Fluka) was used as the oil phase. *n*-Butyl cyanoacrylate was kindly donated by Tong Shen Ent. Co., (Taiwan). Water used for all experiments was doubly distilled and purified by means of Millipore (Bedford, MA) Milli-Q purification system.

2.2. Preparation of microemulsion-based templates

All oil-in-water microemulsions were constructed at a 1:1 surfactant-to-cosurfactant weight ratio according to directions given in (Wilk et al., 2009; Zielinska et al., 2008a). The samples were prepared by diluting surfactant:cosurfactant/oil (or surfactant/oil) and cyanine mixtures with water. After each addition of water fraction samples were vigorously shaken and left for 24 h to attain equilibrium. Samples were checked by both visual observations, and by inspection with a polarizing light microscope (Olympus CX 41, Japan) to identify the non-birefringent system. The type of microemulsion (o/w and w/o or bicontinuous) was evaluated by means of its conductivity which was measured using an EMU Universal Electrochemical Meter fitted with a platinum electrode. These measurements were carried out during the titration of the starting mixtures of the surfactant, cosurfactant, and oil (or water) with water (or oil) through different dilution lines. The electrode was dipped in the microemulsion sample until equilibrium was reached. Reproducibility was checked for certain samples and no significant differences were observed.

2.2. Preparation of loaded nanocapsules

n-Butyl cyanoacrylate (BCA) monomer (1.4 mg/mL, 3.6 mg/mL or 7.2 mg/mL concentrations) dissolved in chloroform (20 – 90 µl) was slowly added to 4 ml of selected microemulsion containing IR-768, IR-780 or IR-783. Interfacial polymerization was performed at 4ºC and the system was stirred for at least 4 hours to complete the synthesis. The pH of the microemulsion was adjusted to either 2.0 or over 5.0 using hydrochloric acid and sodium hydroxide. Then the nanocapsules were collected by centrifugation at 10,000 rpm for 15 min at 25°C (Eppendorf Centrifuge, Unipen 310 rotor) and the thus obtained nanospheres were dispersed in PBS solution. The entrapment efficiency (E) of cyanines in the PBCA nanocapsules was determined as previously described by Graf (Graf et al.,2008; Graf et al., 2009), which is based on the method of Watnasirichaikul (Watnasirichaikul et al. 2000a). Entrapment of IR-768, IR-780 and IR-783 was determined indirectly by measuring the concentration of the remaining cyanine in the supernatant following the isolation of the nanoparticles. The difference between the mass of cyanine solubilized in the polymerization template and the unloaded amount measured in the supernatant of the resulting nanocapsule dispersion following centrifugation at 12,000 rpm for 1h at 25ºC. A Metertech SP8001 spectrophotometer with 1 cm path length quartz thermostated cell was used to determine the amount of the photosensitizer encapsulation in nanocapsules by detecting the concentration of the remaining cyanine in the supernatant following the isolation process of the nanoparticles. All measurements were

performed in triplicate. Cyanine IR-768 was detected at 768 nm, IR-780 at 780 nm and IR-783 at 783 nm. The obtained nanospheres were dispersed in the PBS solution.

2.3. Dynamic light scattering (DLS)

The particle size and distribution of both the o/w microemulsions, and the PBCA nanocapsules were performed according to directions given in (Zielinska et al., 2008a; Zielinska et al., 2008b) with a Zetasizer Nano ZS from Malvern Instruments with a new non-invasive back scatter (NIBS) technology in order to determine the size and polydispersity of the droplets. They were carried out at the scattering angle of 173º with an apparatus equipped with a He–Ne laser (632.8 nm) and an ALV 5000 multibit multitau autocorrelator; the number of counts in the autocorrelation decay was always greater than 10. The droplet's mean diameter was computed by the Stokes–Einstein's law: $R_H = k_BT/(6\pi\eta D)$, where R_H, k_B, T, η, and D are the hydrodynamic radius of the droplet, Boltzmann's constant, temperature in Kelvin, viscosity and diffusion constant, respectively. The DTS (Nano) program was applied for the data evaluation. In the case of the nanocapsules, residual oil and surfactant were removed by repeated washing in ethanol and centrifugation at 10,000 rpm for 15 min at 25°C and then the dry nanocapsules were dispersed in propylene glycol for the DLS measurement.

2.4. Atomic force microscopy (AFM)

A total of 20 µL of ethanol suspension of the nanoparticles was deposited on a freshly cleaned mica surface, which corresponded to an approximate surface concentration of about 10 molecules/µm^2. The samples were then dried overnight. Imaging was carried out using ultra-low amplitude tapping mode on Veeco NanoScope Dimension V AFM, with a with a RT ESP Veeco tube scanner. Scanning speed was 0.5 Hz, and a low resonance frequency pyramidal silicon cantilever resonating at 250-331 kHz was used (force constant = 20-80 N/m).

2.5. Scanning electron microscopy (SEM)

The external structure of the dry nanocapsules was visualized by a scanning electron microscope (Jeol, JSM-5800 LV), in which ethanol dispersions of the nanocapsules were placed on the sample holder, the ethanol was allowed to evaporate, and the nanocapsules were coated with carbon. The samples were viewed at an accelerating voltage of 22 kV.

2.6. Absorption spectroscopy

Absorption measurements of cyanines dissolved in tetrahydrofuran:water (THF:water 1:1, v/v) as well as empty and loaded PBCA nanocapsules dispersed in THF:water were made on a Metertech SP8001 SP 2101 UV–Vis spectrophotometer with 1 cm path length thermostated quartz cell.

3. RESULTS AND DISCUSSION

Chemical structures of the studied cyanine-type photosensitizers along with their abbreviations are shown in Fig.1.

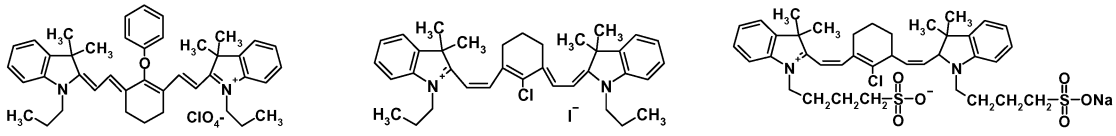

IR-768 IR-780 IR-783

Fig. 1. The selected hydrophobic cyanines.

The hydrophobic cyanines designated as the photosensitizer are absorbed by all cells and selectively retained by malignant tissue. After light exposition the molecule is promoted to an excited state and induces local release of

cytotoxic reactive oxygen species (ROS). Depending on the experimental conditions and cell sensitivity, the cytotoxic molecular species resulting from PDT may trigger cell apoptosis or induce necrosis (Almeida et al., 2004). In clinical PDT some side effects are observed as a result of the dark toxicity of photosensitizers towards normal tissues. Low dark toxicity is one of the important criteria for assessing the usefulness of photosensitizers (Castano et al., 2004).

The main approach to obtaining the oil-cored nanocapsules is the preparation and characterization of o/w microemulsions stabilized by the selected nonionics polyoxyethylene 20 sorbitan monooleate (Tween 80) and polyoxyethylene 10 oleyl ether (Brij 96), the most commonly used surfactants in pharmaceutical applications due to their high biocompatibility and low cytotoxicity and irritancy (Thadros, 2005; Lawrence and Rees, 2000). *Iso*-propyl myristate (IPM) was employed as pharmaceutically oriented oil phase (Lawrence and Rees, 2000). Additional requirements of microemulsions for applications in the preparation of oil-cored nanocapsules are that the dispersed droplets must be oil and the microemulsion must be satisfactorily fluid to permit good mixing following addition of the monomer. Selected o/w microemulsions containing 10% emulsifier (surfactant or surfactant with cosurfactant), 5% oil, and 85% water (R_H equaled to 9.5 and 12.8 nm, respectively for Brij 96 and Tween 80 microemulsions) were applied in our studies for the transcriptive synthesis of PBCA nanocapsules by interfacial polymerization using *n*-butyl cyanoacrylate as the reactive monomer at 1.4 mg/mL, 3.6 mg/mL or 7.2 mg/mL concentrations. Characteristics of poly(*n*-butyl cyanoacrylate) hollow nanoparticles (PBCA) prepared in miroemulsion-templated polymerizations are shown in Table 1 where S denotes the selected surfactant, Co – the cosurfactant, Ol – the oil phase.

Table 1. Characteristics of poly(*n*-butyl cyanoacrylate) loaded hollow nanoparticles prepared by o/w microemulsion–templated processes

System*	microemulsions			loaded nanocapsules								
				IR-768			IR-780			IR-783		
	S	Co	Ol	R_H [nm]	PdI	E [%]	R_H [nm]	PdI	E [%]	R_H [nm]	PdI	E [%]
1a				171.7	0.19	89.4	184.6	0.37	61.1	158.1	0.18	74.8
1b	Tween 80	IP	IPM	254.7	0.27	89.5	384.5	0.62	60.9	221.3	0.39	75.0
1c				394.6	0.43	88.5	420.0	0.65	65.8	351.3	0.62	77.3
2a				124.6	0.25	73.7	111.2	0.19	80.1	134.3	0.19	87.9
2b	Brij 96	-	IPM	159.7	0.46	79.1	136.1	0.30	86.9	148.6	0.37	88.5
2c				202.5	0.39	82.3	180.9	0.35	86.5	195.5	0.45	90.1

* the monomer concentrations for 1a and 2a was 1.4 mg/mL; for 1b and 2b - 3.6 mg/mL; for 1c and 2c - 7.2 mg/mL

Generally the polydispersity index (PdI, calculated according to the ISO 1332 international standard on dynamic light scattering) is defined as the ratio of size deviation (or width of distribution) to mean particle diameter (Sun, 2004). A polydispersity index of 1 indicates large variations in particle size; a reported value of 0 means that the size variation is absent. The obtained PdI values, varying from 0.18 to 0.65 and from 0.19 to 0.46, respectively, for Tween 80/IP/IPM/water and Brij 96/IPM/water nanocapsules, indicated some differences in the homogeneity of the reported oil-cored nanoparticle population, but nanocapsules prepared with relatively low monomer contents (mainly systems 1a and 2a) for which PdI $\leq$ 0.3 were quite monodisperse according to (Pereira et al., 2008; Watnasirichaikul et al., 2000b).

The diameter of the obtained nanocapsules was dependent on the template applied and the monomer amount used for the polymerization. The particle size ranged from 111 to 420 nm ± 2.5 nm and did not differ for unloaded and cyanine – IR-768, IR-780, IR-783-loaded nanoparticles. Moreover, the mean particle sizes were not significantly different between the different microemulsion templates. The size of the obtained nanoparticles was the most desirable and our results corresponded well with other reports (Gaumet et al., 2008; Krauel et al., 2005).

Nanoparticle size is considered one of the most significant parameters in the uptake of particles by cells (Gaumet et al., 2008; Krauel et al., 2005). The size of nanoparticles influences the biodistribution activity as nanometer-range particles have easy accessibility in the body, being transported via the circulation to different body sites. Particles which are too small are removed from the circulation by renal filtration, while larger ones may undergo

scavenging by the reticuloendothelial system. The most accessible nanoparticles for PDT use should have diameters much below 1 μm (Bechet et al., 2008) thus the nanoproducts fabricated in the present study fulfill the size requirement, especially since the polymerization of *n*-butyl cyanoacrylate has been found to produce biodegradable polymers (Leonard et al., 1966).

The percentage of the cyanines incorporation was achieved in the range of 60-90% (see Table 1) as a result of the amount of *n*-butyl cyanoacrylate used for polymerization. It is similar to the case of insulin, being encapsulated in water-in-oil systems (Watnasirichaikul et al., 2002). The type of microemulsion template slightly influenced the cyanines entrapment level and it was higher for nanocapsules prepared from Brij 96 microemulsion templates. Additionally, the cyanine entrapment efficiency was enhanced with the increase in *n*-butyl cyanoacrylate monomer concentration used in microemulsion-template polymerization (Table 1) and such results correspond with previous reports related to, for example, curcuminoids and insulin delivered in PBCA nanocapsules (Watnasirichaikul et al., 2002; Graf et al., 2009). The preparation of nanocapsules from oil-in-water microemulsions as reported in the present contribution results in a high encapsulation efficiency of hydrophobic cyanines since the oil-soluble dye is devoted to the oil phase which is in the form of nanodroplets of the oil-in-water microemulsions. Polymerization at the oil/water interface can thus encapsulate a large amount of the hydrophobic photosensitizers.

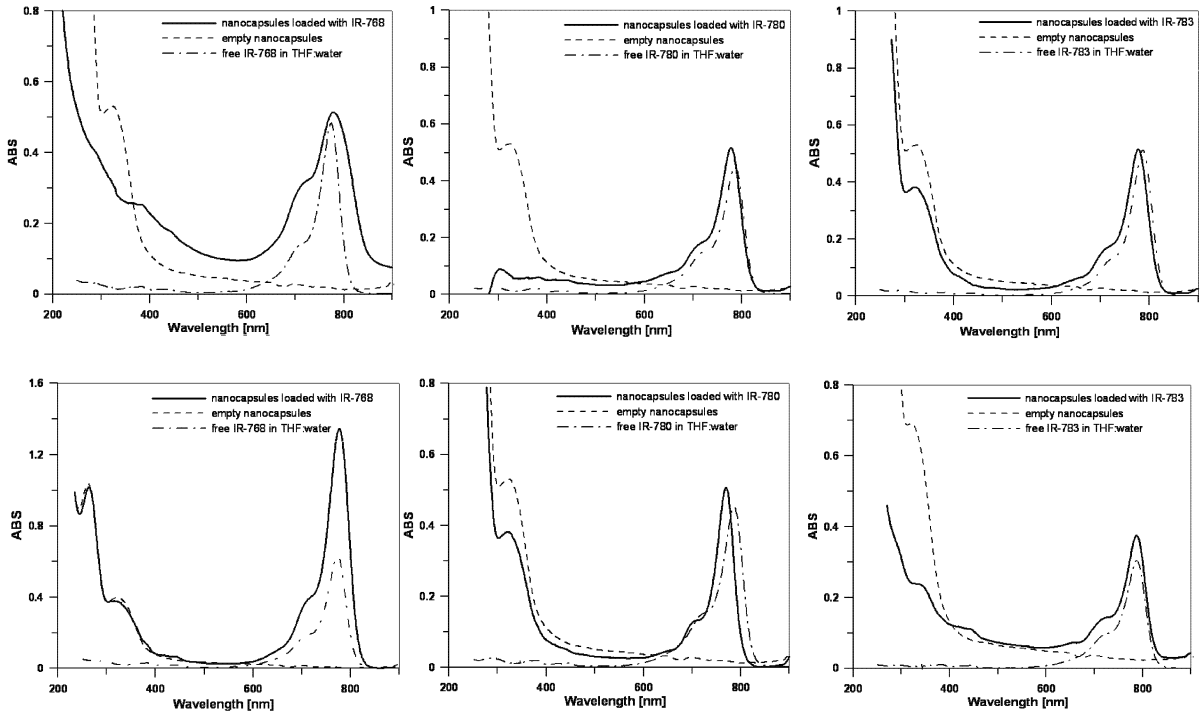

Fig. 2. Absorption spectra in a THF:water solution of the Tween 80/IP/IPM/water nanocapsules (according to system 1b in Table 1) – upper part and Brij 96/IPM/water nanocapsules (according to system 2b in Table 1) in relation to respective cyanine.

The investigated cyanines diluted in THF:water exhibit a strong absorbance in the red region as in (Kassab, 2002), with a maximum wavelength at 775, 786 and 789 nm for IR-768, IR-780 and IR-783 respectively. The results presented in Figure 2 show that selected photosensitizers loaded in nanocapsules do not suffer changes in photophysical properties after the encapsulation process, as it has also been described for poly(D,L lactic-co-glycolic acid) nanoparticles containing phtalocyanine (Ricci-Júnior et al., 2006).

Free cyanines and loaded nanocapsules have similar photophysical behaviors, so these results show that encapsulation process is suitable and these can be treated as direct evidence of the hydrophobic photosensitizer encapsulation. Additionally nanocapsules from both o/w microemulsion templates have high encapsulation efficiency. The preparation of nanocapsules from both ternary (Brij 96/IPM/water) and pseudoternary (Tween 80/IP/IPM/water) o/w microemulsion templates as described in the present report results in a high encapsulation

efficiency of cyanines IR-768, IR-780 and IR-783. The free cyanines are poorly soluble in aqueous media, with macroscopic undissolved flakes of the compound visible in the solution. In contrast, the entrapment of photosenthitizers within the microemulsions and nanocapsules allowed one to obtain a clear and dispersed formulation with a hue derived from the natural color of the green dye.
The obtained cyanine loaded nanocapsules are usually spherical in shape when viewed with AFM (Fig. 3, scan sizes shown in the figures) and SEM (Fig. 4). Moreover, no differences in their morphology were visualized for particles from various types of microemulsion structure. It was found that the surface of the nanocapsules (see SEM images in Fig. 4) is smooth without pores. The morphology of the majority of the nanocapsules appeared similar to the example shown in Figure 3 and 4.

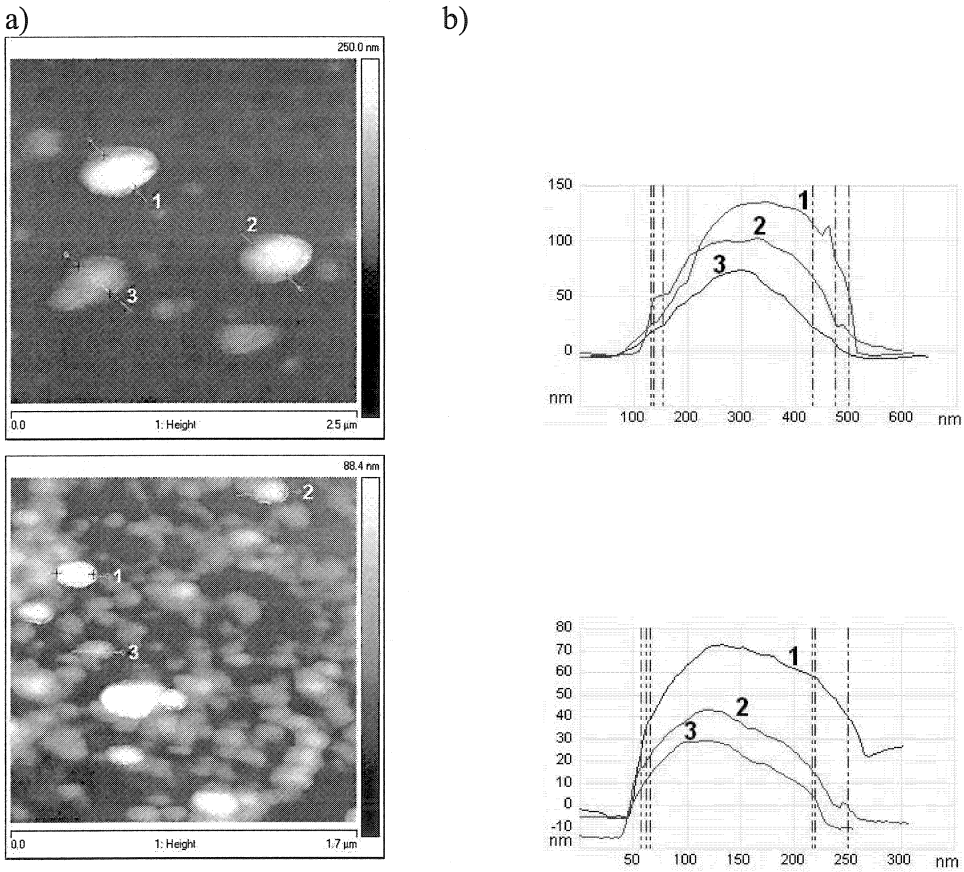

Fig. 3. Morphology of nanocapsules loaded with IR-780 based on Tween 80/IP/IPM/water (according to system 1b in Table 1) – upper part and Brij 96/IPM/water (according to system 2b in Table 1) – lower data. (a) AFM images, (b) cross sections.

The cross sections produced by the AFM (see Fig. 3b), what present a heterogeneous distribution in size and height of obtained PBCA nanocapsules. The diameter/height ratios were calculated from the AFM nanocapsules profiles (Fig. 3b). The values showed a ratio of approximately 10 for both types of loaded nanocapsules. These results confirmed the existence of flattened forms that were also suggested by Leite (2005) who prepared poly-ε-caprolactone nanocapsules with a diameter/height ratio of 10. Similarly, Montasser (2002) observed a ratio of approximately 12 for the co-polymer dichlorophthaoyl-co-diethylenetriamine capsules. Possible nanocapsules flattening and aggregation process can take place after drying on mica surface and it is probably related to variations in polymeric wall thickness.
While DLS measures hydrodynamic radius, the microscopy techniques (AFM and SEM) allows direct measurement of size in samples in a dried state, which permits simultaneous characterization of particle shape and structure. The horizontal widths of nanocapsules determined by AFM are shown in Figure 3b, and these data

indicate a nanocapsule diameter of about 170 nm and 160 nm for Tween 80 and Brij 96 templated capsules respectively. Similarly, the average size of nanocapsules estimated from SEM was about 160 nm (Fig. 4a). Therefore, both AFM and SEM give nanocapsule sizes in good agreement with the sizes obtained from the DLS method. Some differences regarding nanocapsules' sizes between DLS and microscopy data are due to hydration of the particles in solution when measured by DLS and/or shrinking of the capsules during the drying approach in the sample preparation for SEM.

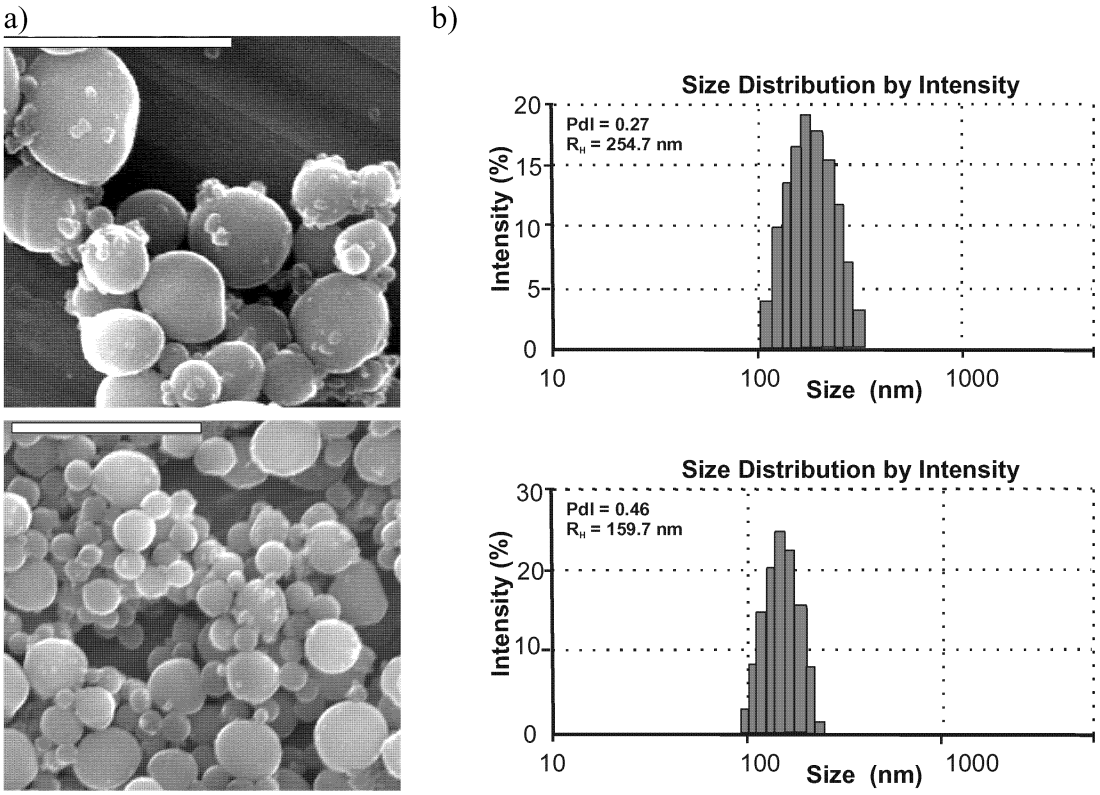

Fig. 4. SEM micrographs and DLS size distributions of the IR-780 - nanocapsules based on the following systems: Tween 80/IP/IPM/water (according to system 1b in Table 1) – upper part and Brij 96/IPM/water (according to system 2b in Table 1) – lower data. Scale 500 nm.

4. CONCLUSIONS

Ternary and pseudoternary systems containing nonionic surfactants (Tween 80 and Brij 96) and the , *iso*-propanol (as the cosurfactant) *iso*-propylmyristate (as the oil phase) can be used as nanoparticle templates for the incorporation of hydrophobic cyanine-type photosensitizers using a one-step preparation method by interfacial polymerization providing easy processing and scaling-up possibilities. The results obtained will be useful for our further investigations on biodegradable nanocapsules and their release characteristics as useful photosensitizer delivery systems in the PDT of some cancers. No differences in their morphology were visualized for the loaded nanoparticles formed from various types of templates. The size of the studied nanocapsules was found to be a function of the microemulsion type and ratio of the monomer mass used for the polymerization process (thickness of the polymeric wall).

5. ACKNOWLEDGEMENTS

This work was financially supported by the Polish Ministry of Science and Higher Education (Grant No. N205013854).

6. REFERENCES

Allemann E., Gurny R. and Doelker E. (1993). *Eur. J. Pharm. Biopharm*., 39, 173
Almeida R.D., Manadas B.J., Carvalho A.P. and Duarte C.B. (2004). *Biochim. Biophys. Acta*., 1704, 59
Bechet, D., Couleand, P., Frochot, C., Viriot, M.L., Guillemin, F., Barbieri-Heyob, M. (2008). *Trends in Biotechnol*. 26, 612
Castano A.P., Demidova T.N. and Hamblin M.R. (2004). *Photodagn. Photodyn. Ther*., 1, 279
Couvreur P., Barratt G., Fattal E., Legrand P. and Vautier C. (2002). *Crit. Rev. Ther. Drug Carrier Syst.,* 19, 99
Crescenzi E., Varriale, L. Iovino M. and Chiaviello A., Veneziani, B.M., Palumbo, G. (2004). *Mol.Cancer Ther.,* 3, 537
Date A.A. and Nagarsenker M.S. (2008). *Int. J. Pharm*., 355, 19
Gasco M.R. and Trotta M. (1986). *Int. J. Pharm.,* 29, 267
Gaumet M., Vargas A., Gurny R. and Delie F. (2008). *Eur. J. Pharm. Biopharm*., 69, 1
Graf, A., Jack, K.S., Whittaker, A.K., Hook, S.M., Rades, T. (2008). *Eur. J. Pharm. Sci*. 33, 434
Graf, A., Rades, T., Hook, S.M. (2009). *Eur. J. Pharm. Sci*. 37, 53
Guterres S.S., Alves M.P. and Pohlmann A.R. (2007). *Drug Target Insights,* 2, 147
International Standard ISO 13321, Particle size analysis, Part 8: Photon Correlation Spectroscopy, *International Organization of Standardization*, 1996
Kassab K. (2002). *J. Photochem. Photobiol. B: Biology*, 68, 15
Krauel K., Davies N.M., Hook S. and Rades T. (2005). *J. Control. Release*, 106, 76
Lawrence, M.J., Rees, G.D. (2000). *Adv. Deliv. Rev*. 45, 89
Leite E.A. , Vilela J.M.C., Mosqueira V.C.F., Spangler Andrade M. (2005). *Microsc. Microanal*. 11, 48
Leonard, F., Kulkarni, R.K., Brandes, G., Nelson, J., Cameron, J.J. (1966). *J. Applied Polym. Sci*. 10, 259
Montasser I, Fessi H., Coleman A.W. (2002) *Eur. J. Pharm. Biopharm.* 54 281
Pereira M.A., Mosqueira V.C., Vilela J.M., Andrade M.S., Romaldes, Cardoso V.N. (2008). *Eur. J. Pharm. Sci*. 33, 42
Ricci-Júnior E., Marchetti J.M. (2006). *Int. J. Pharm*. 310, 187
Sun Z., Sevick-Muraca E.M. (2004). J. Colloid Interface Sci. 270, 329
Thadros, T.F. (2005). Surfactants in Pharmaceutical Formulations. In: Applied Surfactants. Principles and Applications. WILEY-VCH Verlag GmbH & Co. KGaA, Weinheim, pp. 433-502
Wang C., Ye W., Zheng Y., Liu X., Tong Z. (2007). *Int. J. Pharm.*, 338, 165
Watnasirichaikul S., Davies N.M., Rades T., Tucker I.G. (2000a). *Pharm. Res*. 17,684
Watnasirichaikul S., Rades T., Tucker I.G. and Davies N.M. (2002). *Int. J. Pharm.*, 235, 237
Wilk K.A., Zielinska K., Agnieszka Hamerska-Dudra, Jezierski A. (2009). *J. Colloid Interface Sci.*, 334, 87
Zielinska K., Wilk K.A., Jezierski A., Jesionowski T. (2008a). *J. Colloid Interface Sci.*, 321, 408
Zielinska K., Wilk K.A. Seweryn E., Pietkiewicz J. and Saczko J. (2008b). *Material Sci. Poland*, 26 (2), 443